Mori et al. Virology Journal 2014, 11:11
http://www.virologyj.com/content/11/1/11

VIROLOGY JOURNAL

RESEARCH Open Access

Replication interference between human papillomavirus types 16 and 18 mediated by heterologous E1 helicases

Seiichiro Mori*, Rika Kusumoto-Matsuo, Yoshiyuki Ishii, Takamasa Takeuchi and Iwao Kukimoto

Abstract

Background: Co-infection of multiple genotypes of human papillomavirus (HPV) is commonly observed among women with abnormal cervical cytology, but how different HPVs interact with each other in the same cell is not clearly understood. A previous study using cultured keratinocytes revealed that genome replication of one HPV type is inhibited by co-existence of the genome of another HPV type, suggesting that replication interference occurs between different HPV types when co-infected; however, molecular mechanisms underlying inter-type replication interference have not been fully explored.

Methods: Replication interference between two most prevalent HPV types, HPV16 and HPV18, was examined in HPV-negative C33A cervical carcinoma cells co-transfected with genomes of HPV16 and HPV18 together with expression plasmids for E1/E2 of both types. Levels of HPV16/18 genome replication were measured by quantitative real-time PCR. Physical interaction between HPV16/18 E1s was assessed by co-immunoprecipitation assays in the cell lysates.

Results: The replication of HPV16 and HPV18 genomes was suppressed by co-expression of E1/E2 of heterologous types. The interference was mediated by the heterologous E1, but not E2. The oligomerization domain of HPV16 E1 was essential for HPV18 replication inhibition, whereas the helicase domain was dispensable. HPV16 E1 co-precipitated with HPV18 E1 in the cell lysates, and an HPV16 E1 mutant Y379A, which bound to HPV18 E1 less efficiently, failed to inhibit HPV18 replication.

Conclusions: Co-infection of a single cell with both HPV16 and HPV18 results in replication interference between them, and physical interaction between the heterologous E1s is responsible for the interference. Heterooligomers composed of HPV16/18 E1s may lack the ability to support HPV genome replication.

Keywords: Human papillomavirus, Co-infection, Replication, Interference, E1 helicase

Background

Human papillomavirus (HPV) has a circular double-stranded DNA genome of approximately 8 kilo base-pairs packaged in a capsid composed of two proteins L1 and L2 [1]. HPVs are classified into at least 170 types based on the homology of nucleotide sequences of the L1 gene [2], among which HPV16 and HPV18 are responsible for approximately 70% of cervical cancer cases worldwide.

The life cycle of HPV is tightly linked to the differentiation of host epithelial cells. HPV infects basal cells of stratified epithelia through small lesions, in which the viral genome is maintained as episomes without expressing capsid genes and is passed on to daughter cells. When the host cells initiate epithelial differentiation, the HPV genome starts to replicate, and infectious virions are produced and released from terminally differentiated cornified cells [3].

Productive replication of the HPV genome in differentiated cells requires a viral DNA helicase E1, a viral replication/transcription factor E2, and a replication origin DNA, containing specific binding sites for E1 (E1BS)

* Correspondence: moris@nih.go.jp
Pathogen Genomics Center, National Institute of Infectious Diseases, 4-7-1 Gakuen, Musashi-murayama, Tokyo 208-0011, Japan

BioMed Central

© 2014 Mori et al.; licensee BioMed Central Ltd. This is an Open Access article distributed under the terms of the Creative Commons Attribution License (http://creativecommons.org/licenses/by/2.0), which permits unrestricted use, distribution, and reproduction in any medium, provided the original work is properly cited. The Creative Commons Public Domain Dedication waiver (http://creativecommons.org/publicdomain/zero/1.0/) applies to the data made available in this article, unless otherwise stated.

and E2 (E2BS) [4]. To initiate viral genome replication, E2 binds to the E2BS at the origin and recruits E1, leading to the formation of an E1/E2 complex at the replication origin [4]. Then, E1 changes its conformation by binding to ATP, which causes a release of E2 from the origin. After dissociation of E2, E1 assembles into double trimers to unwind double-stranded DNA. The E1 double trimers serve as precursors for subsequent formation of double hexamers that finally function as a processive DNA helicase at replication forks [5].

E1 consists of four domains: an N-terminal domain (ND), a DNA-binding domain (DBD), an oligomerization domain (OD), and a helicase domain (HD) [4]. The ND contains nuclear localization and export signals, and has a regulatory role in viral genome replication, by controlling subcellular localization of E1 [6]. The DBD is required for E1 binding to the E1BS at the replication origin [7,8]. The OD is responsible for E1-oligomerization [9,10]. The HD has nonspecific DNA-binding and ATPase activities, and mediates interaction with E2 [5,7].

Co-infection with multiple HPV types in a single cervical specimen has been reported in 30–45% of HPV-positive women [11-15]. Furthermore, several studies indicate recombination between different HPV types [16-19], which strongly suggests that a single cell can be co-infected with different HPV types in vivo.

A previous study reported that HPV45 genomes are not maintained in cultured keratinocytes co-transfected with genomes of other HPV types, such as HPV18, HPV31, and HPV39 [20]. This study also demonstrated that while HPV31 and HPV39 genomes are stably maintained within the same cell, copy numbers of genomes of both types are extremely low compared to those in cells containing each genotype individually. These observations suggest an interference of genome replication between different HPV types. However, mechanisms underlying the replication interference have not been fully explored.

In this study, to examine simultaneous replication of HPV16 and HPV18 genomes in the same cell, we used a cell-based transient replication assay that has been used to study E1/E2-dependent HPV replication [21-26]. The HPV-negative C33A cervical cancer cell line was co-transfected with HPV16 and HPV18 genomes together with E1/E2 expression plasmids for both types, and levels of genome replication were measured by quantitative real-time PCR. We report replication interference between HPV16 and HPV18, and propose a molecular mechanism of the interference.

Results

Expression of FLAG-tagged E1/E2s of HPV16 and HPV18 in C33A cells

We constructed expression plasmids for FLAG-tagged HPV16 E1 (F16E1), HPV16 E2 (F16E2), HPV18 E1 (F18E1), and HPV18 E2 (F18E2), and named them: pF16E1, pF16E2, pF18E1, and pF18E2, respectively. Figure 1 shows the expression of the FLAG-tagged E1/E2s in HPV-negative C33A cells transiently transfected with different mixtures of pF16E1 and pF16E2, and/or pF18E1 and pF18E2. The E1/E2 proteins of both types were detected by Western blotting with anti-FLAG antibody. The expression levels of E1/E2 of HPV18 were higher than those of HPV16. Although the expression level of HPV16 E2 was extremely low, the level was sufficient to support HPV16 replication (see below).

Replication of HPV16 or HPV18 genomes supported by homologous or heterologous E1/E2s

E1/E2s of HPV16 and HPV18 supported genome replication of both the homologous and heterologous types (Figure 2). C33A cells were transfected with circularized full-genome DNA (gDNA) of HPV16 (Figure 2A) or HPV18 (Figure 2B) together with increasing amounts of pF16E1 and pF16E2, or pF18E1 and pF18E2. Three days after transfection, low molecular weight DNA was isolated using the Hirt procedure, digested with *Dpn*I, and *Dpn*I-resistant HPV gDNA quantified by real-time PCR as previously reported [22,25,26]. The maximum levels of replication for HPV16 and HPV18 genomes were observed when cells were transfected with 40 ng of each

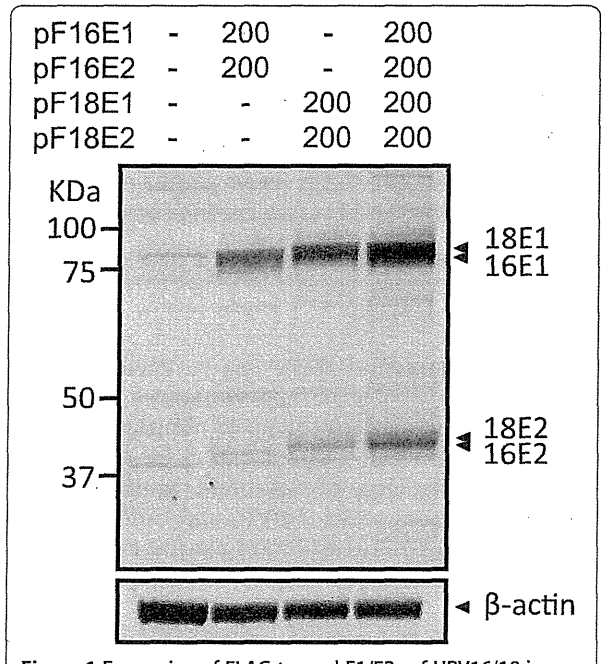

Figure 1 Expression of FLAG-tagged E1/E2s of HPV16/18 in C33A cells. C33A cells were transfected with the indicated amounts (ng) of the expression plasmids for E1/E2s of HPV16/18. Two days after transfection, FLAG-tagged E1/E2s in the cell lysates were detected by Western blotting with anti-FLAG antibody. β-actin was detected as loading control.

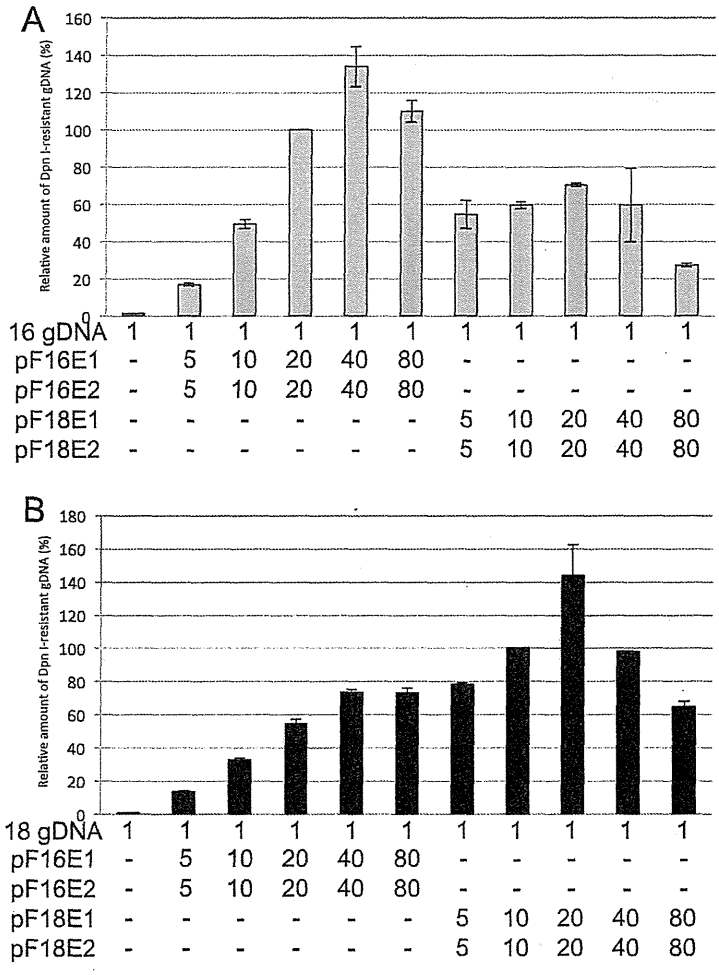

Figure 2 Replication of HPV16 or HPV18 genomes supported by homologous or heterologous E1/E2s. C33A cells were transfected with 1 ng of the HPV16 **(A)** or HPV18 **(B)** gDNAs together with the indicated amounts (ng) of the expression plasmids for E1/E2s. Three days after transfection, low molecular weight DNA was isolated by the Hirt procedure and digested with *DpnI*. The *DpnI*-resistant HPV gDNA was quantified by real-time PCR and normalized to the luciferase gene. The level of the replication was presented as the relative amount of the *DpnI*-resistant DNA compared to that obtained by the replication when cells were transfected 20 ng of each pF16E1 and pF16E2 **(A)** or 10 ng of each pF18E1 and pF18E2 **(B)**. Each bar represents the average of two independent experiments with the standard error of mean.

pF16E1 and pF16E2 and 20 ng of each pF18E1 and pF18E2, respectively. Compared to the replication levels for HPV16 or HPV18 supported by the homologous E1/E2, replication supported by the heterologous E1/E2 was relatively inefficient.

Transfection with excess amounts of the E1/E2 expression plasmids (>80 ng of each pF16E1 and pF16E2, and >40 ng of each pF18E1 and pF18E2) decreased the replication levels for both types (Figure 2) and increased the number of detached cells (data not shown). Since E1 is known to activate a cellular DNA damage response, which results in delayed S phase [27,28], overexpression of E1 may be toxic for C33A cells and reduce the replication efficiency. Therefore, in later experiments, we transfected cells with suboptimal amounts of the expression plasmids (<20 ng of each pF16E1 and pF16E2, and <10 ng of each pF18E1 and pF18E2).

Simultaneous replication of HPV16 and HPV18 genomes in the presence of E1/E2s of both types

Replication of HPV16 and HPV18 genomes was suppressed by co-expression of the heterologous E1/E2 (Figure 3). C33A cells were transfected with a mixture of gDNAs and E1/E2 expression plasmids for both types to mimic simultaneous replication of HPV16 and HPV18 genomes in a co-infected cell. When cells were transfected with 20 ng of each pF16E1 and pF16E2 together with 10 ng of each pF18E1 and pF18E2, the replication levels of both types were reduced to around 20%. The inhibitory effect of HPV18 E1/E2 on HPV16

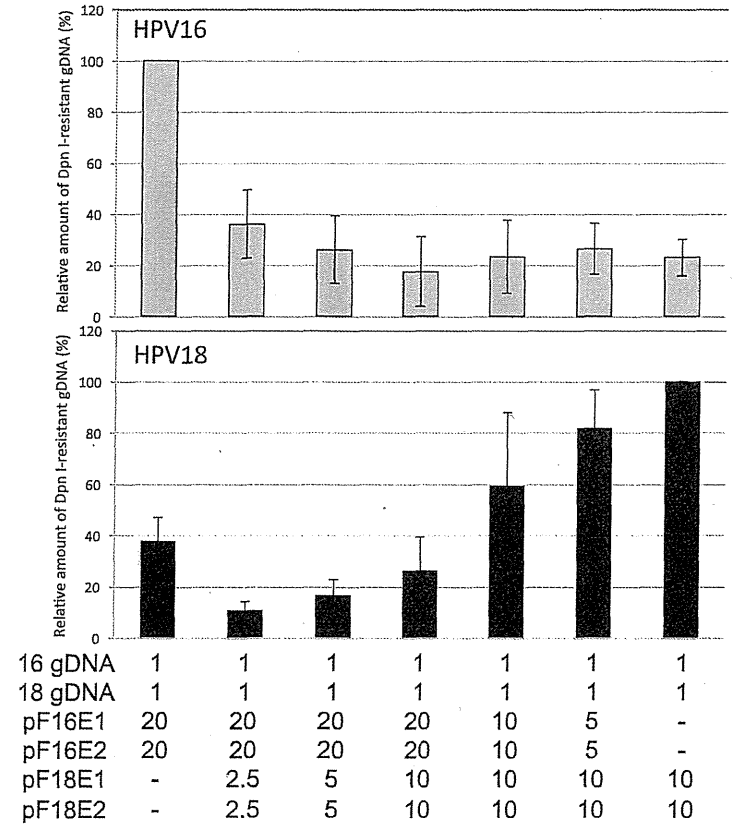

Figure 3 Simultaneous replication of HPV16/18 genomes in the presence of E1/E2s of both types. C33A cells were transfected with a mixture of HPV16 and HPV18 gDNAs (1 ng each) together with the indicated amounts (ng) of the expression plasmids. Three days after transfection, low molecular weight DNA was isolated by the Hirt procedure and digested with *Dpn*I. The *Dpn*I-resistant HPV16 (upper panel) and HPV18 (lower panel) gDNAs were quantified by real-time PCR and normalized to the luciferase gene. The level of the replication was presented as the relative amount of the *Dpn*I-resistant DNA compared to that obtained by the replication with the homologous E1/E2 alone. Each bar represents the average of three independent experiments with the standard deviation.

replication was more pronounced than that of HPV16 E1/E2 on HPV18 replication.

Effects of heterologous E1 or E2 on HPV16/18 replication

The heterologous E1, but not E2 inhibited HPV16 and HPV18 replication (Figure 4). HPV18 E1 inhibited HPV16 replication to the level observed in the presence of E1/E2s of both types (Figure 4A). The same was true for HPV16 E1 in HPV18 replication inhibition (Figure 4B). These results clearly indicate that the replication interference between HPV16 and HPV18 is mediated by the heterologous E1, not by E2.

Effects of HPV16 E1 mutants on HPV18 replication

To examine which functional domain of HPV16 E1 is responsible for the inhibition of HPV18 replication, we constructed expression plasmids for deletion mutants of HPV16 E1 (Figure 5A), and tested their capability to inhibit HPV18 replication.

As shown in Figure 5B, the OD of HPV16 E1 was essential for the inhibition of HPV18 replication, whereas the HD is dispensable. A deletion mutant F16E1-439, which lacks the HD, inhibited HPV18 replication as efficiently as full-length F16E1. In contrast, deletion mutants F16E1-359 and F16E1-184 failed to inhibit HPV18 replication. As expected, all of the deletion mutants completely lost the ability to support HPV16 replication (data not shown). Furthermore, an amino-acid substitution mutant F16E1-Y379A, which is supposed to negate the ability of E1 to oligomerize on single-stranded DNA and to bind to the replication origin [9,29], did not inhibit HPV18 replication. These results indicate that the OD of HPV16 E1 is responsible for the observed reduction in HPV18 replication efficiency.

Physical interaction between E1s of HPV16/18 in C33A cells

The requirement of the OD of HPV16 E1 for the inhibition of HPV18 replication strongly suggests that a

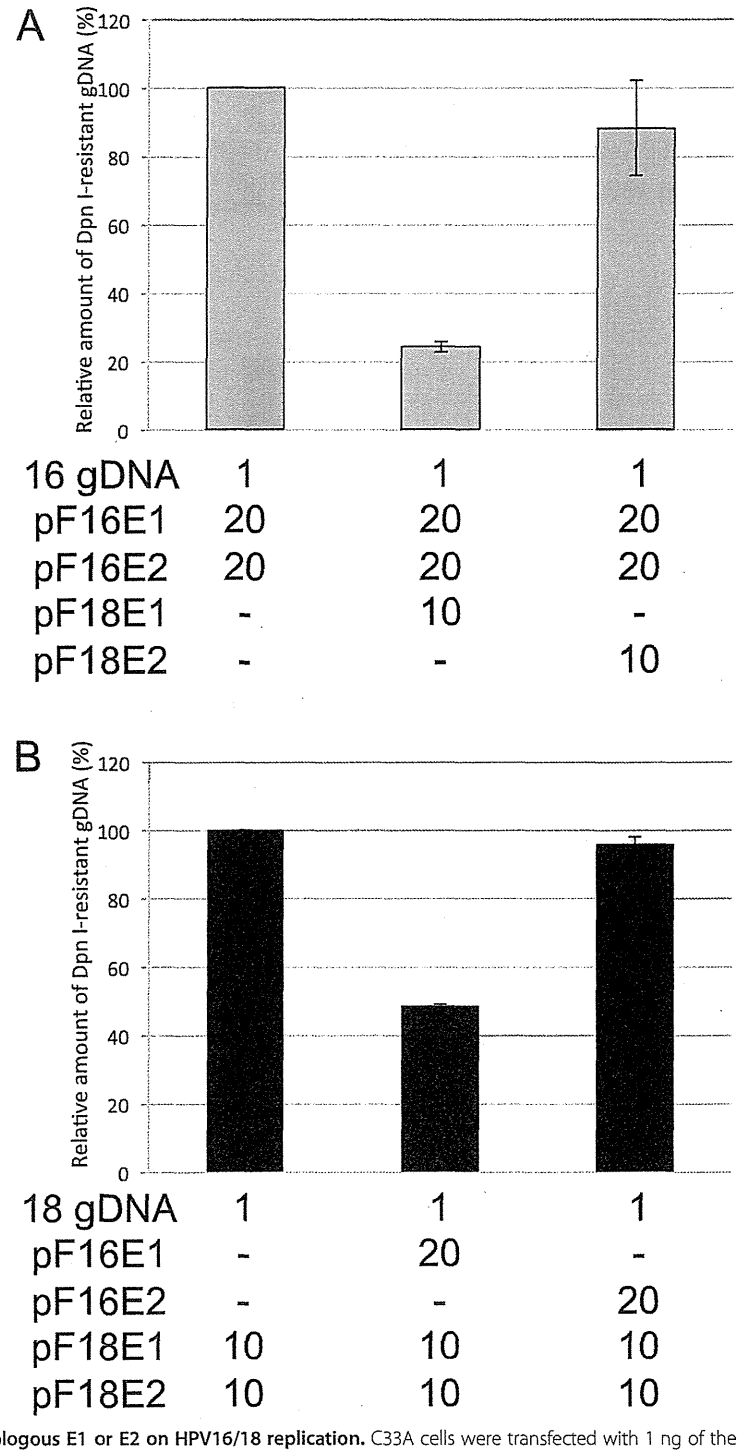

Figure 4 Effects of heterologous E1 or E2 on HPV16/18 replication. C33A cells were transfected with 1 ng of the HPV16 **(A)** or HPV18 **(B)** gDNAs together with the indicated amounts (ng) of the expression plasmids for E1/E2s. Three days after transfection, low molecular weight DNA was isolated by the Hirt procedure and digested with *DpnI*. The *DpnI*-resistant HPV gDNA was quantified by real-time PCR and normalized to that of the luciferase gene. The level of the replication was presented as the relative amount of the *DpnI*-resistant DNA compared to that obtained by the replication with the homologous E1/E2 alone. Each bar represents the average of two independent experiments with the standard error of mean.

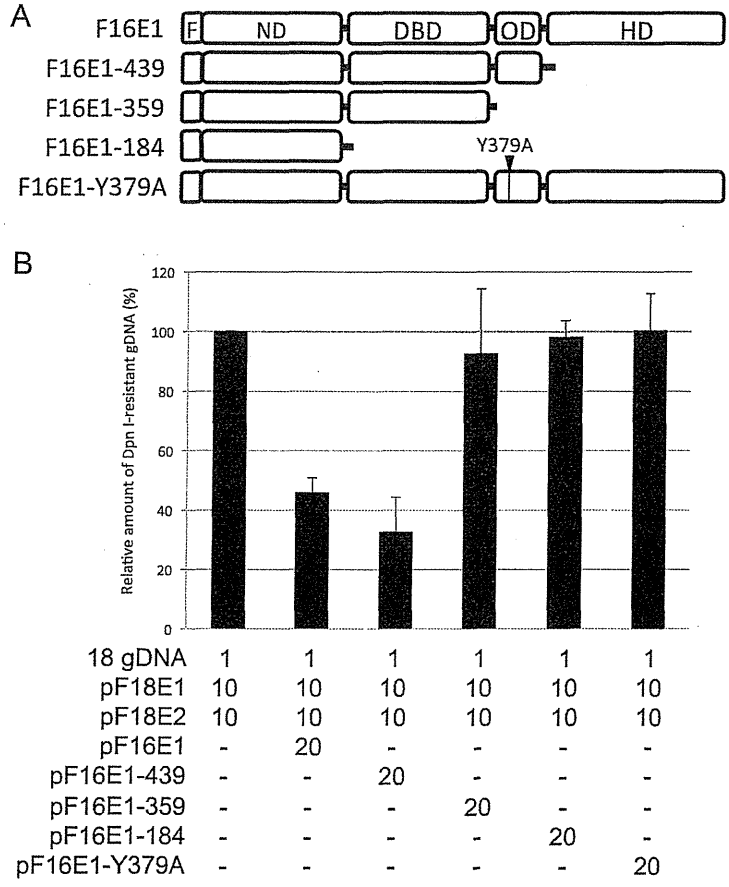

Figure 5 Effects of HPV16 E1 mutants on HPV18 replication. (A) Schematic representation of HPV16 E1 mutants. F, FLAG-tag; ND, N-terminal domain; DBD, DNA-binding domain; OD, oligomerization domain; HD, helicase domain. **(B)** C33A cells were transfected with 1 ng of the HPV18 gDNA together with the indicated amounts (ng) of the expression plasmids. Three days after transfection, low molecular weight DNA was isolated by the Hirt procedure and digested with *DpnI*. The *DpnI*-resistant HPV18 gDNA was quantified by real-time PCR and normalized to the luciferase gene. The level of the replication was presented as the relative amount of the *DpnI*-resistant DNA compared to that obtained by the replication with the HPV18 E1/E2 alone. Each bar represents the average of two independent experiments with the standard error of mean.

physical interaction between the heterologous E1s is involved in the interference. Thus, we examined the interaction between E1s of HPV16 and HPV18 using co-immunoprecipitation assays. C33A cells were transfected with HPV18 gDNA together with expression plasmids for hexahistidine (6×His)-tagged HPV18 E1 (pH18E1), untagged HPV18 E2 (p18E2), and each of the HPV16 E1 mutants described above. Two days after transfection, F16E1 in cell lysates was immunoprecipitated with anti-FLAG antibody, followed by detection of H18E1 co-precipitated with F16E1 by Western blotting with anti-6×His antibody. H18E1 efficiently co-precipitated with F16E1 in the cell lysate (Figure 6A). Similarly H18E1 co-precipitated with F16E1 in the absence of HPV18 E2 and gDNA (Figure 6B), suggesting that the interaction is direct and not mediated by either HPV18 E2 or gDNA. H18E1 bound less efficiently to F16E1-439 and F16E1-359, but not to F16E1-184 (Figure 6A). Importantly, the OD mutant, F16E1-Y379A, showed reduced binding efficiency compared to F16E1.

The direct interaction between E1s of HPV16 and HPV18 was further confirmed by using purified E1 proteins: 6xHis-tagged HPV16 E1 (H16E1) and FLAG-tagged HPV18 E1 (F18E1). H16E1 was incubated with F18E1, and F18E1 in the mixture was immunoprecipitated with anti-FLAG antibody, followed by Western blotting with anti-6×His antibody. Clearly H16E1 co-precipitated with F18E1 (Figure 6C), indicating that HPV16 E1 directly binds to HPV18 E1.

Taken together, these results strongly suggest that HPV16 E1 interacts with HPV18 E1 through the region containing the DBD, OD, and HD, and that the OD is an important determinant for efficient interaction.

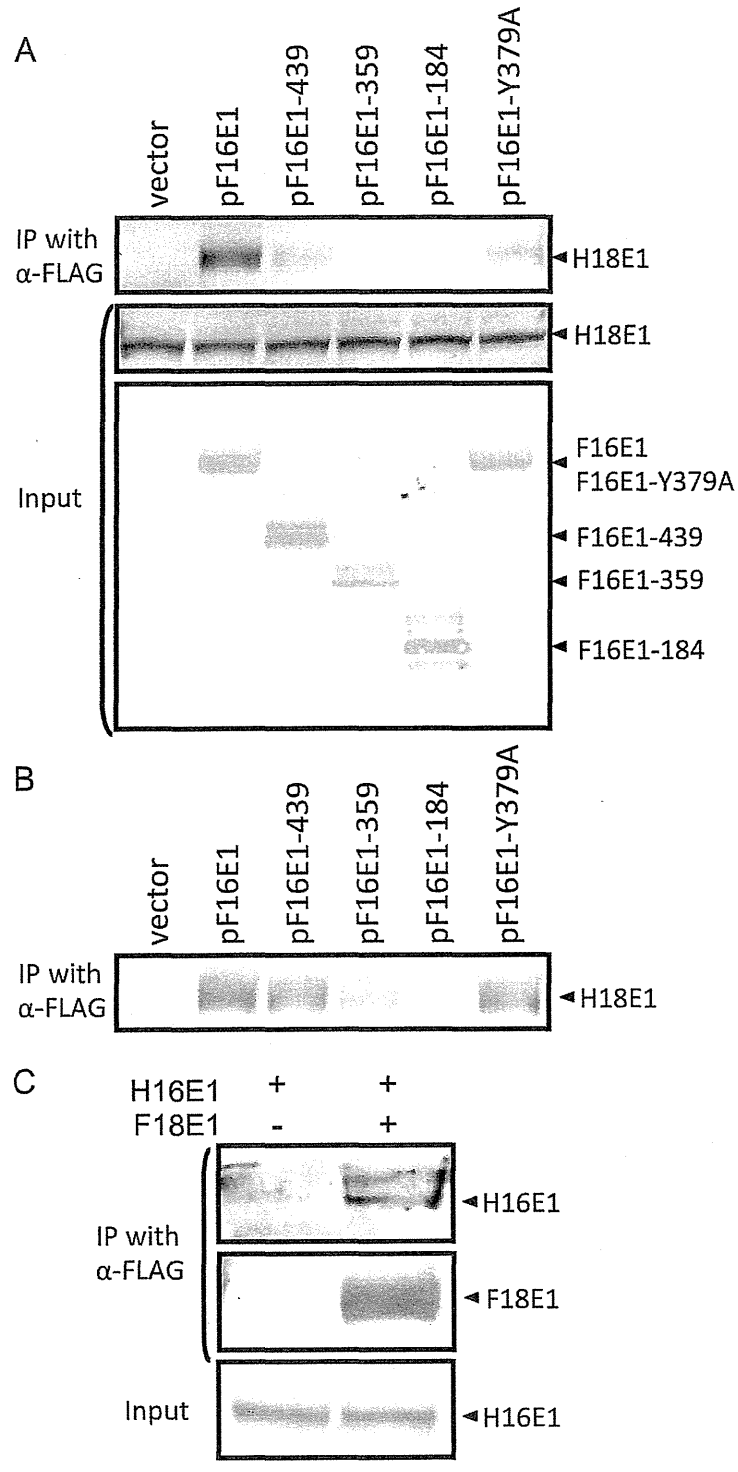

Figure 6 (See legend on next page.)

(See figure on previous page.)
Figure 6 Interaction between E1s of HPV16/18. (A) C33A cells were transfected with the HPV18 gDNA together with the expression plasmids for hexahistidine (6xHis)-tagged HPV18 E1 (pH18E1), the untagged HPV18 E2 (p18E2), and one of the FLAG-tagged HPV16 E1 mutants. Two days after transfection, the FLAG-tagged HPV16 E1s in cell lysates were immunoprecipitated with anti-FLAG antibody, and HPV18 E1 co-precipitated with HPV16 E1s was detected by Western blotting with anti-6xHis antibody (upper panel). HPV18 E1 (middle panel) and HPV16 E1s (lower panel) in the total cell lysates were detected by Western blotting with anti-6xHis and anti-FLAG antibodies, respectively. **(B)** C33A cells were transfected with pH18E1 and pF16E1 without HPV18 gDNA and p18E2, followed by immunoprecipitation and Western blotting as described above. **(C)** Purified 6xHis-tagged HPV16 E1 (H16E1) was incubated with or without purified FLAG-tagged HPV18 E1 (F18E1), followed by immunoprecipitation with anti-FLAG antibody. H16E1 and F18E1 in the immunoprecipitates were detected by Western blotting with anti-6xHis (upper panel) and anti-FLAG antibodies (middle panel), respectively. H16E1 in the input mixture was visualized with anti-6xHis antibody (lower panel).

Discussion

In this study using cell-based transient replication assays we found replication interference between HPV16 and HPV18 and explored the underlying molecular mechanisms. We examined replication of HPV16/18 genomes under conditions of exogenous expression of E1/E2 for both types from the Cytomegalovirus promoter because expression of E1/E2 from native HPV promoters is too weak to support HPV genome replication in C33A cells. Although these experimental conditions do not necessarily reflect a natural context of HPV transcription, the results obtained in this study provide a novel mechanistic insight into inter-type HPV replication interference, which could not be addressed in the previous study using transfection of HPV genomes alone [20].

The mutational analysis of HPV16 E1 indicates that the OD, which is responsible for the E1-E1 interaction [9,10], is essential for the inhibition of HPV18 replication. In particular, the inability of the OD mutant F16E1-Y379A to inhibit HPV18 replication strongly implies that the OD-mediated interaction between HPV16 and HPV18 E1s is critical for replication interference. On the other hand, the deletion mutant F16E1-439, which lacks the HD and shows reduced binding (at a similar level to the OD mutant), still retains the capability to inhibit HPV18 replication, suggesting that the binding between HPV16 and HPV18 E1s via the HD does not contribute to the replication interference. Furthermore, because the HD is essential for helicase activity, as well as E1 binding to E2 [30-32], the results clearly indicate that the enzymatic activity of E1 and its binding to E2 are not involved in replication inhibition. It is also worth noting that the replication interference is not simply due to competition between heterologous E1/E2s for origin binding because E1/E2s of HPV16 and HPV18 supported genome replication of heterologous types (Figure 2).

A comparison of amino acid sequences between HPV16 and HPV18 E1s reveals that the OD is the most conserved region between the two (Figure 7A). The amino acid identities in the ND, DBD, OD, and HD are 46, 60, 66, and 64% homologous, respectively (Figure 7B). The high sequence similarity observed between ODs strongly supports the possibility of heterooligomer formation between the two types. Collectively, these results implicate E1 heterooligomer formation via the OD as the molecular mechanism behind replication inhibition.

We propose a model in which HPV16 and HPV18 E1 heterooligomers do not have proper configurations and are deficient in the ability to support genome replication for both HPV16 and HPV18. Since the amino acid sequence in the ND is less conserved between HPV16 and HPV18 E1s (Figure 7), it may exert a negative effect on the replication activities of E1 heterooligomers, although the exact functions of the ND in the conformation of E1 homooligomers are not yet well understood. Alternatively, it is possible that the E1 heterooligomers are unable to bind efficiently to the replication origin or unwind double-stranded DNA, and/or that they are deficient in recruiting cellular factors required for HPV replication, such as DNA polymerase alpha [34], replication protein A [35], and topoisomerase I [36].

Serological studies have shown that seropositivities for HPV6 and HPV11 significantly antagonize the development of HPV16-related cervical cancer [37,38]. Interestingly, these studies also demonstrated a tendency for antagonistic interactions between HPV16 and HPV18. Seropositivity for HPV18 reduces the risk of HPV16-related cervical cancer, although statistical significance was not achieved. Although the underlying mechanism of such serological interaction is not clear, interference of genome replication between HPV16 and other HPV types may be involved, as observed in this study. It is unlikely that antibodies against HPV6, HPV11, or HPV18 capsids protect women from infection with HPV16, because antisera against these types do not cross-neutralize HPV16 in vitro [39]. It will thus be of interest to investigate whether HPV6 and HPV11 interfere with HPV16 replication in transient replication assays such as those described here.

Interference between multiple HPV types has been also proposed in several pathological studies. Genomes of different HPV types were detected in distinct, non-overlapping areas of the same genital tissue by in situ hybridization [40-42]. When cervical tumor biopsies, in which genomes of both HPV16 and HPV18 were detected by PCR, were analyzed by fluorescence in situ hybridization, the integrated form of either HPV16 or

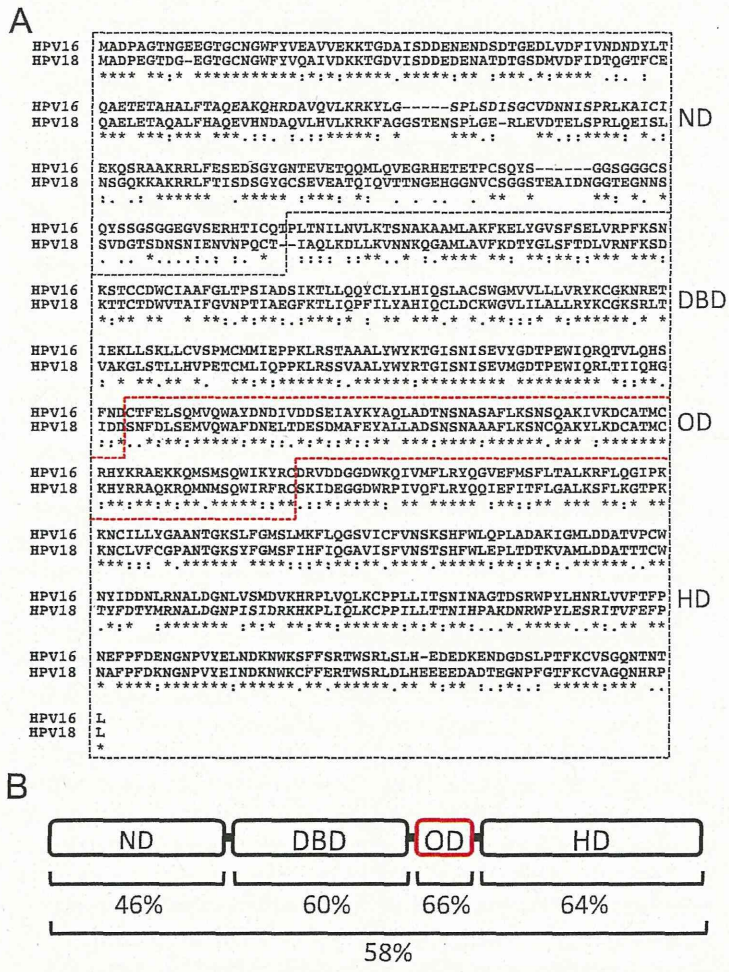

Figure 7 Amino acid sequence similarity between HPV16/18 E1s. (A) The amino acid sequence alignment between HPV16/18 E1s using MAFFT [33]. Identical residues are indicated with asterisks (*). Highly conserved residues are indicated with colons (:). Semi-conserved residues are indicated with periods (.). **(B)** The amino acid sequence identities of the ND (amino acids 1 to 190 of HPV16 E1 and 1 to 197 of HPV18 E1), DBD (amino acids 191 to 352 of HPV16 E1 and 198 to 359 of HPV18 E1), OD (amino acids 353 to 430 of HPV16 E1 and 360 to 437 of HPV18 E1), HD (amino acids 431 to 649 of HPV16 E1 and 438 to 657 of HPV18 E1), or the entire regions (amino acids 1 to 649 of HPV16 E1 and 1 to 657 of HPV18 E1) between HPV16/18 E1s are presented.

HPV18 was detected in an individual cell [43]. Although the genomes of HPV1 and HPV63 were detected in the same cell of a plantar wart, only a cytopathogenic effect typical of HPV63 infection was seen in the cell [44].

Our experimental results and previous observations reported by others indicate that interactions between different HPV types during their life cycle may affect the propagation, pathogenesis, and evolution of HPVs.

Conclusions

This study indicates that co-infection of a single cell with HPV16 and HPV18 results in replication interference between them, and that interaction between the heterologous E1s is responsible for the interference.

Materials and methods

Plasmids and HPV genomes

The codon-optimized E1 and E2 genes of HPV16 and HPV18 were synthesized by Life Technologies (Carlsbad, CA, USA) and cloned into the *Not*I site of pCMV, which had been created by removing the β-galactosidase gene from pCMVβ (Clontech, Mountain View, CA, USA). The FLAG-tag sequence was added to the 5′-terminus of each gene in pCMV by using PCR to produce pF16E1, pF16E2, pF18E1, and pF18E2. The 6xHis-tag sequence was added to the 5′-terminus of the HPV18 E1 gene in pCMV to produce pH18E1. A stop codon was introduced into pF16E1 by using PCR to produce expression plasmids for HPV16 E1 deletion mutants; pF16E1-439, pF16E1-359, and pF16E1-184 express

amino acid (aa) 2 to 439, aa 2 to 359, and aa 2 to 184 of the HPV16 E1, respectively. The codon 379 of the E1 gene in pF16E1 was changed from TAC to GCA by using PCR to produce pF16E1-Y379A, which expresses HPV16 E1 with amino acid substitution of tyrosine to alanine at aa residue 379.

The circularized HPV16 and HPV18 gDNAs were prepared by in vitro self-ligation of linear viral genomes. The full-length genomes of HPV16 and HPV18 were released from the cloned vector pUC18 by digestion with *Bam*HI and *Eco*RI, respectively. The linearized genomes were incubated with T4 DNA ligase at final concentration 2.5 μg/ml of DNA for overnight at 4°C. The ligated DNAs were purified and concentrated by using the QIAprep Spin Miniprep Kit (Qiagen GmbH, Hilden, Germany).

Cell culture

C33A cervical carcinoma cells were cultured in Dulbecco's modified minimal essential medium (DMEM) supplemented with 10% fetal bovine serum (FBS) and grown in 5% CO_2 at 37°C.

Western blot

C33A cells (1×10^6 cells) were grown in a 6-well plate for 6 h and then transfected with the expression plasmids for FLAG-tagged E1/E2 of HPV16/18 using the FuGene HD (Roche Diagnostics, Indianapolis, IN, USA). Two days after transfection the cells were lysed in SDS-sample buffer, followed by boiling of the cell lysate for 5 min. The extracted proteins were separated by SDS-PAGE and transferred to a PVDF membrane (Life Technologies). After blocking the membrane with phosphate-buffered saline (PBS) containing 0.02% Tween-20 and 5% skimmed milk, FLAG-tagged E1/E2s were probed with rabbit polyclonal anti-FLAG antibody (Sigma-Aldrich Co. St. Louis, Mo, USA) and horseradish peroxidase conjugated anti-rabbit IgG goat antibody (Santa Cruz Biotechnology, Inc., Santa Cruz, CA, USA). The immunoreactive proteins were visualized using the Pierce Western Blotting Substrate Plus (Thermo Fisher Scientific Inc. Waltham, MA, USA) and the Typhoon 9410 Image Scanner (GE Healthcare, Piscataway, NJ, USA).

Transient replication assay

C33A cells (2×10^5 cells) were grown in a 24-well plate for 6 h and then transfected with HPV gDNAs and the expression plasmids for E1/E2 together with 1 ng of pGL3-Basic (Promega, Madison, WI, USA), which lacks a replication origin for HPV, using the FuGene HD. The total amount of transfected DNA was adjusted to 400 ng with the empty vector, pCMV. The next day of the transfection, the medium was changed to DMEM containing 10% FBS. Three days after transfection low molecular weight DNA was isolated by the Hirt procedure. Briefly, 200 μl of lysis solution (10 mM Tris–HCl [pH 8.0], 10 mM EDTA [pH 8.0], and 1% SDS) was added to the cells, followed by cell lysis for 10 min at room temperature with gentle agitation. Fifty μl of 5 M NaCl was then added to the cell lysate, and incubated overnight at 4°C. The mixture was centrifuged at 50,000 × g for 30 min at 4°C to precipitate proteins and genomic DNA of the cells. The HPV gDNAs were isolated from the supernatant using the QIAamp DNA Blood Mini Kit (Qiagen GmbH), and eluted with 50 μl of elution buffer (10 mM Tris–HCl [pH 8.0] and 1 mM EDTA). To digest the transfected DNA, 2 μl of the DNA sample was incubated with 10 U of *Dpn*I in 20 μl of 1 × reaction buffer (New England Biolabs, Ipswich, MA, USA) for 2 h at 37°C, followed by heat inactivation of *Dpn*I at 80°C for 20 min. The amounts of *Dpn*I-resistant HPV16/18 gDNAs were quantified by real-time PCR with HPV16/18 type-specific primers and SYBR-green dye. Total 20 μl of a PCR reaction mixture containing 2 μl of the *Dpn*I-digested sample, 10 μl of SYBR Green Realtime PCR Master Mix (TOYOBO CO., LTD, Osaka, Japan), and 0.4 μM of each primer was subjected to real-time PCR analysis using the LightCycler 480 (Roche Diagnostics). The nucleotide sequences of primers are as follows: forward primer for HPV16, 5′-CACCTCCAGCACCTAAAGAA; reverse primer for HPV16, 5′-TTGC GTCCTAAAGGAAACTG; forward primer for HPV18, 5′-GATGTGAGAAACACACCACA; reverse primer for HPV18, 5′-GCAGTGAAGTGTTCAGTTCC; forward primer for the luciferase gene, 5′-AGGCGAACTGTGTGT GAGAG; reverse primer for the luciferase gene, TTCA GGCGGTCAACGATGAA. Each amplicon of the HPV16/18 genomes contains two *Dpn*I sites, whereas that of the luciferase gene has no *Dpn*I site. The amounts of *Dpn*I-resistant HPV gDNA were normalized to those of the luciferase gene.

Immunoprecipitation

C33A cells (1×10^6 cells) were grown in a 6-well plate for 6 h and then transfected with HPV18 gDNA, pH18E1, and p18E2, together with one of the expression plasmids for HPV16 E1 mutants, using the FuGene HD. Two days after transfection the cells were lysed in 100 μl of RIPA buffer (25 mM Tris–HCl [pH7.6], 150 mM NaCl, 1% NP-40, 1% sodium deoxycholate, and 0.1% SDS), followed by centrifugation of the cell lysate at 10,000 × g for 10 min at 4°C. The supernatant was diluted 4-fold with PBS, and precleared with 20 μl of Dynabeads protein G magnetic beads (Life Technologies) for 30 min at 4°C. The precleared lysate was further incubated with 2 μg of the rabbit polyclonal anti-FLAG antibody (Sigma-Aldrich Co.) and 20 μl of the protein G magnetic beads for 2 h at 4°C. The beads were then

washed with PBS containing 0.02% Tween-20 four times, and the bound proteins were eluted by boiling the beads in 20 μl of SDS-sample buffer. The recovered proteins were resolved by SDS-PAGE and transferred to a PVDF membrane. 6×His-tagged HPV18 E1 on the membrane was probed by mouse monoclonal anti-6×His antibody (Qiagen GmbH) and detected with horseradish peroxidase conjugated anti-mouse IgG goat antibody (Santa Cruz Biotechnology, Inc.) as described above.

6×His-tagged HPV16 E1 (H16E1) protein was prepared from bacterial cells. Briefly, the H16E1 gene was cloned into pET-30 (Novagen, Madison, WI, USA), and the H16E1 protein was purified from *Escherichia coli* BL21(DE3) pLysS that had been transformed with the expression plasmid as described previously [45]. FLAG-tagged HPV18 E1 (F18E1) protein was prepared from insect cells by using the baculovirus expression system (Life Technologies). Briefly, the F18E1 gene was cloned into pFastBac1 (Life Technologies), and the resultant plasmid was introduced into *E. coli* DH10Bac-competent cells (Life Technologies) to obtain recombinant Bacmid DNA. A recombinant baculovirus expressing F18E1 was produced in Sf9 cells transfected with the recombinant Bacmid DNA. The F18E1 protein was purified from Sf9 cells that had been infected with the recombinant baculovirus as described previously [45]. For binding reaction, 1 μg of H16E1 and 4 μg of F18E1 were diluted with 200 μl of binding buffer (20 mM Tris–HCl [pH8.0], 150 mM NaCl, 2 mM MgCl2, and 0.01% NP-40), and incubated with 4 μl of the rabbit polyclonal anti-FLAG antibody (Sigma-Aldrich Co.) and 15 μl of the protein G magnetic beads (Life Technologies) for 1 h at 4°C. The beads were then washed with the binding buffer four times, and the bound proteins were analyzed by Western blotting as described above.

Abbreviations

HPV: Human papillomavirus; E1BS: E1 binding site; E2BS: E2 binding site; ND: N-terminal domain; DBD: DNA-binding domain; OD: Oligomerization domain; HD: Helicase domain; aa: Amino acid; DMEM: Dulbecco's modified minimal essential medium; FBS: Fetal bovine serum; PBS: Phosphate-buffered saline.

Competing interests

The authors declare that they have no competing interests.

Authors' contributions

SM and IK designed this study and drafted the manuscript. SM performed experiments. RKM and IK technically supported the experiments. SM, RKM, YI, TT, and IK revised the manuscript critically. All authors have read and approved the final manuscript.

Acknowledgments

We thank Dr. Tadahito Kanda (Center of Research Network for Infectious Diseases, Riken, Tokyo, Japan) for critical reading of the manuscript. This work was supported by a grant-in-aid from the Ministry of Health, Labour and Welfare for the Third-Term Comprehensive 10-year Strategy for Cancer Control.

Received: 26 November 2013 Accepted: 21 January 2014
Published: 24 January 2014

References

1. Howley PM, Lowy DR: **Papillomaviruses and their replication.** In *Fields Virology Volume 2.* 4th edition. Edited by Lnipe DM, Howley PM. Philadelphia: Lippincott, Williams and Wilkins; 2001:2197–2229.
2. de Villiers EM: **Cross-roads in the classification of papillomaviruses.** *Virology* 2013, **445**:2–10.
3. Longworth MS, Laimins LA: **Pathogenesis of human papillomaviruses in differentiating epithelia.** *Microbiol Mol Biol Rev* 2004, **68**:362–372.
4. McBride AA: **Replication and partitioning of papillomavirus genomes.** *Adv Virus Res* 2008, **72**:155–205.
5. Schuck S, Stenlund A: **Assembly of a double hexameric helicase.** *Mol Cell* 2005, **20**:377–389.
6. Deng W, Lin BY, Jin G, Wheeler CG, Ma T, Harper JW, Broker TR, Chow LT: **Cyclin/CDK regulates the nucleocytoplasmic localization of the human papillomavirus E1 DNA helicase.** *J Virol* 2004, **78**:13954–13965.
7. Sarafi TR, McBride AA: **Domains of the BPV-1 E1 replication protein required for origin-specific DNA binding and interaction with the E2 transactivator.** *Virology* 1995, **211**:385–396.
8. Thorner LK, Lim DA, Botchan MR: **DNA-binding domain of bovine papillomavirus type 1 E1 helicase: structural and functional aspects.** *J Virol* 1993, **67**:6000–6014.
9. Titolo S, Pelletier A, Pulichino AM, Brault K, Wardrop E, White PW, Cordingley MG, Archambault J: **Identification of domains of the human papillomavirus type 11 E1 helicase involved in oligomerization and binding to the viral origin.** *J Virol* 2000, **74**:7349–7361.
10. Enemark EJ, Joshua-Tor L: **Mechanism of DNA translocation in a replicative hexameric helicase.** *Nature* 2006, **442**:270–275.
11. Gravitt PE, Peyton CL, Alessi TQ, Wheeler CM, Coutlée F, Hildesheim A, Schiffman MH, Scott DR, Apple RJ: **Improved amplification of genital human papillomaviruses.** *J Clin Microbiol* 2000, **38**:357–361.
12. Coutlée F, Gravitt P, Kornegay J, Hankins C, Richardson H, Lapointe N, Voyer H, Franco E: **Use of PGMY primers in L1 consensus PCR improves detection of human papillomavirus DNA in genital samples.** *J Clin Microbiol* 2002, **40**:902–907.
13. van Doorn LJ, Quint W, Kleter B, Molijn A, Colau B, Martin MT, Kravang-In, Torrez-Martinez N, Peyton CL, Wheeler CM: **Genotyping of human papillomavirus in liquid cytology cervical specimens by the PGMY line blot assay and the SPF (10) line probe assay.** *J Clin Microbiol* 2002, **40**:979–983.
14. Klug SJ, Hukelmann M, Hollwitz B, Düzenli N, Schopp B, Petry KU, Iftner T: **Prevalence of human papillomavirus types in women screened by cytology in Germany.** *J Med Virol* 2007, **79**:616–625.
15. Kondo K, Uenoyama A, Kitagawa R, Tsunoda H, Kusumoto-Matsuo R, Mori S, Ishii Y, Takeuchi T, Kanda T, Kukimoto I: **Genotype distribution of human papillomaviruses in Japanese women with abnormal cervical cytology.** *Open Virol J* 2012, **6**:277–283.
16. Narechania A, Chen Z, DeSalle R, Burk RD: **Phylogenetic incongruence among oncogenic genital alpha human papillomaviruses.** *J Virol* 2005, **79**:15503–15510.
17. Varsani A, van der Walt E, Heath L, Rybicki EP, Williamson AL, Martin DP: **Evidence of ancient papillomavirus recombination.** *J Gen Virol* 2006, **87**:2527–2531.
18. Angulo M, Carvajal-Rodríguez A: **Evidence of recombination within human alpha-papillomavirus.** *Virol J* 2007, **28**:33.
19. Gottschling M, Stamatakis A, Nindl I, Stockfleth E, Alonso A, Bravo IG: **Multiple evolutionary mechanisms drive papillomavirus diversification.** *Mol Biol Evol* 2007, **24**:1242–1258.
20. McLaughlin-Drubin ME, Meyers C: **Evidence for the coexistence of two genital HPV types within the same host cell in vitro.** *Virology* 2004, **321**:173–180.
21. Chiang CM, Ustav M, Stenlund A, Ho TF, Broker TR, Chow LT: **Viral E1 and E2 proteins support replication of homologous and heterologous papillomaviral origins.** *Proc Natl Acad Sci USA* 1992, **89**:5799–5803.
22. Taylor ER, Morgan IM: **A novel technique with enhanced detection and quantitation of HPV-16 E1- and E2-mediated DNA replication.** *Virology* 2003, **315**:103–109.
23. Wang XM, Jansen KU, McClements WL: **DNA replicative functions of highly-expressed, codon-optimized human papillomavirus proteins E1 and E2.** *J Virol Methods* 2003, **108**:83–90.

24. Lin BY, Broker TR, Chow LT: **Analysis of HPV DNA replication using transient transfection and cell-free assays.** *Methods Mol Med* 2005, **119**:331–348.
25. Morgan IM, Taylor ER: **Detection and quantitation of HPV DNA replication by Southern blotting and real-time PCR.** *Methods Mol Med* 2005, **119**:349–362.
26. Kukimoto I, Mori S, Sato H, Takeuchi T, Kanda T: **Transcription factor human Skn-1a enhances replication of human papillomavirus DNA through the direct binding to two sites near the viral replication origin.** *FEBS J* 2008, **275**:3123–3135.
27. Sakakibara N, Mitra R, McBride AA: **The papillomavirus E1 helicase activates a cellular DNA damage response in viral replication foci.** *J Virol* 2011, **85**:8981–8995.
28. Fradet-Turcotte A, Bergeron-Labrecque F, Moody CA, Lehoux M, Laimins LA, Archambault J: **Nuclear accumulation of the papillomavirus E1 helicase blocks S-phase progression and triggers an ATM-dependent DNA damage response.** *J Virol* 2011, **85**:8996–9012.
29. Titolo S, Brault K, Majewski J, White PW, Archambault J: **Characterization of the minimal DNA binding domain of the human papillomavirus e1 helicase: fluorescence anisotropy studies and characterization of a dimerization-defective mutant protein.** *J Virol* 2003, **77**:5178–5191.
30. Yasugi T, Benson JD, Sakai H, Vidal M, Howley PM: **Mapping and characterization of the interaction domains of human papillomavirus type 16 E1 and E2 proteins.** *J Virol* 1997, **71**:891–899.
31. Masterson PJ, Stanley MA, Lewis AP, Romanos MA: **A C-terminal helicase domain of the human papillomavirus E1 protein binds E2 and the DNA polymerase alpha-primase p68 subunit.** *J Virol* 1998, **72**:7407–7419.
32. Sun Y, Han H, McCance DJ: **Active domains of human papillomavirus type 11 E1 protein for origin replication.** *J Gen Virol* 1998, **79**:1651–1658.
33. Katoh K, Standley DM: **MAFFT multiple sequence alignment software version 7: improvements in performance and usability.** *Mol Biol Evol* 2013, **30**:772–780.
34. Park P, Copeland W, Yang L, Wang T, Botchan MR, Mohr IJ: **The cellular DNA polymerase alpha-primase is required for papillomavirus DNA replication and associates with the viral E1 helicase.** *Proc Natl Acad Sci USA* 1994, **91**:8700–8704.
35. Loo YM, Melendy T: **Recruitment of replication protein A by the papillomavirus E1 protein and modulation by single-stranded DNA.** *J Virol* 2004, **78**:1605–1615.
36. Clower RV, Fisk JC, Melendy T: **Papillomavirus E1 protein binds to and stimulates human topoisomerase I.** *J Virol* 2006, **80**:1584–1587.
37. Silins I, Wang Z, Avall-Lundqvist E, Frankendal B, Vikmanis U, Sapp M, Schiller JT, Dillner J: **Serological evidence for protection by human papillomavirus (HPV) type 6 infection against HPV type 16 cervical carcinogenesis.** *J Gen Virol* 1999, **80**:2931–2936.
38. Luostarinen T, af Geijersstam V, Bjørge T, Eklund C, Hakama M, Hakulinen T, Jellum E, Koskela P, Paavonen J, Pukkala E, Schiller JT, Thoresen S, Youngman LD, Dillner J, Lehtinen M: **No excess risk of cervical carcinoma among women seropositive for both HPV16 and HPV6/11.** *Int J Cancer* 1999, **80**:818–822.
39. White WI, Wilson SD, Bonnez W, Rose RC, Koenig S, Suzich JA: **In vitro infection and type-restricted antibody-mediated neutralization of authentic human papillomavirus type 16.** *J Virol* 1998, **72**:959–964.
40. Nuovo GJ, Darfler MM, Impraim CC, Bromley SE: **Occurrence of multiple types of human papillomavirus in genital tract lesions. Analysis by in situ hybridization and the polymerase chain reaction.** *Am J Pathol* 1991, **138**:53–58.
41. Hinrichs S, Smith L, Ghazvini S, Kirven K, Palladino H, Spaulding D: **Multiple HPV infection: microanatomy by in situ hybridization and immunohistochemistry.** *Mod Pathol* 1992, **5**:257–261.
42. Christensen ND, Koltun WA, Cladel NM, Budgeon LR, Reed CA, Kreider JW, Welsh PA, Patrick SD, Yang H: **Coinfection of human foreskin fragments with multiple human papillomavirus types (HPV-11, -40, and -LVX82/MM7) produces regionally separate HPV infections within the same athymic mouse xenograft.** *J Virol* 1997, **71**:7337–7344.
43. Vermeulen CF, Jordanova ES, Szuhai K, Kolkman-Uljee S, Vrede MA, Peters AA, Schuuring E, Fleuren GJ: **Physical status of multiple human papillomavirus genotypes in flow-sorted cervical cancer cells.** *Cancer Genet Cytogenet* 2007, **175**:132–137.
44. Egawa K, Shibasaki Y, de Villiers EM: **Double infection with human papillomavirus 1 and human papillomavirus 63 in single cells of a lesion displaying only an human papillomavirus 63-induced cytopathogenic effect.** *Lab Invest* 1993, **69**:583–588.
45. Kusumoto-Matsuo R, Kanda T, Kukimoto I: **Rolling circle replication of human papillomavirus type 16 DNA in epithelial cell extracts.** *Genes Cells* 2011, **16**:23–33.

doi:10.1186/1743-422X-11-11
Cite this article as: Mori *et al.*: Replication interference between human papillomavirus types 16 and 18 mediated by heterologous E1 helicases. *Virology Journal* 2014 11:11.

Submit your next manuscript to BioMed Central and take full advantage of:

- **Convenient online submission**
- **Thorough peer review**
- **No space constraints or color figure charges**
- **Immediate publication on acceptance**
- **Inclusion in PubMed, CAS, Scopus and Google Scholar**
- **Research which is freely available for redistribution**

Submit your manuscript at
www.biomedcentral.com/submit

BioMed Central

OPEN ACCESS Freely available online

PLOS | ONE

Genetic Variation of Human Papillomavirus Type 16 in Individual Clinical Specimens Revealed by Deep Sequencing

Iwao Kukimoto[1*☯], Tomohiko Maehama[2☯], Tsuyoshi Sekizuka[1], Yumiko Ogasawara[1], Kazunari Kondo[3], Rika Kusumoto-Matsuo[1], Seiichiro Mori[1], Yoshiyuki Ishii[1], Takamasa Takeuchi[1], Toshiyuki Yamaji[2], Fumihiko Takeuchi[1], Kentaro Hanada[2], Makoto Kuroda[1]

1 Pathogen Genomics Center, National Institute of Infectious Diseases, Tokyo, Japan, 2 Department of Biochemistry and Cell Biology, National Institute of Infectious Diseases, Tokyo, Japan, 3 NTT Medical Center Tokyo, Tokyo, Japan

Abstract

Viral genetic diversity within infected cells or tissues, called viral quasispecies, has been mostly studied for RNA viruses, but has also been described among DNA viruses, including human papillomavirus type 16 (HPV16) present in cervical precancerous lesions. However, the extent of HPV genetic variation in cervical specimens, and its involvement in HPV-induced carcinogenesis, remains unclear. Here, we employ deep sequencing to comprehensively analyze genetic variation in the HPV16 genome isolated from individual clinical specimens. Through overlapping full-circle PCR, approximately 8-kb DNA fragments covering the whole HPV16 genome were amplified from HPV16-positive cervical exfoliated cells collected from patients with either low-grade squamous intraepithelial lesion (LSIL) or invasive cervical cancer (ICC). Deep sequencing of the amplified HPV16 DNA enabled *de novo* assembly of the full-length HPV16 genome sequence for each of 7 specimens (5 LSIL and 2 ICC samples). Subsequent alignment of read sequences to the assembled HPV16 sequence revealed that 2 LSILs and 1 ICC contained nucleotide variations within E6, E1 and the non-coding region between E5 and L2 with mutation frequencies of 0.60% to 5.42%. In transient replication assays, a novel E1 mutant found in ICC, E1 Q381E, showed reduced ability to support HPV16 origin-dependent replication. In addition, partially deleted E2 genes were detected in 1 LSIL sample in a mixed state with the intact E2 gene. Thus, the methods used in this study provide a fundamental framework for investigating the influence of HPV somatic genetic variation on cervical carcinogenesis.

Citation: Kukimoto I, Maehama T, Sekizuka T, Ogasawara Y, Kondo K, et al. (2013) Genetic Variation of Human Papillomavirus Type 16 in Individual Clinical Specimens Revealed by Deep Sequencing. PLoS ONE 8(11): e80583. doi:10.1371/journal.pone.0080583

Editor: Robert D. Burk, Albert Einstein College of Medicine, United States of America

Received May 16, 2013; **Accepted** October 4, 2013; **Published** November 13, 2013

Copyright: © 2013 Kukimoto et al. This is an open-access article distributed under the terms of the Creative Commons Attribution License, which permits unrestricted use, distribution, and reproduction in any medium, provided the original author and source are credited.

Funding: This work was supported by Grants-in-Aid for Scientific Research from the Japanese Ministry of Education, Culture, Sports, and Science; by Grants-in-Aid for Scientific Research from the Ministry of Health, Labor, Welfare, and Technology; and by a grant from the Mitsubishi Foundation. The funders had no role in study design, data collection and analysis, decision to publish, or preparation of the manuscript.

Competing interests: The authors have declared that no competing interests exist.

* E-mail: ikuki@niid.go.jp

☯ These authors contributed equally to this work.

Introduction

Human papillomaviruses (HPVs) are small DNA viruses having a circular double-stranded DNA genome of approximately 8-kb, some of which can induce benign and malignant hyper-proliferative lesions in the skin or mucosa [1]. A subset of mucosal HPVs, referred to as high-risk HPVs, are causally related to the development of cervical cancer, among which HPV type 16 (HPV16) accounts for at least 50% of cervical cancer cases worldwide [2]. Mucosal HPVs infect basal cells in the cervix and establish their genomes as extrachromosomal episomes. When infected cells migrate from the basal layer and begin the process of differentiation, viral genome amplification is initiated, followed by the induction of viral capsid expression and the assembly of infectious virions in the upper layers of epithelia [3]. This differentiation-dependent propagation of HPVs can manifest clinically as low-grade squamous intraepithelial lesion (LSIL). In contrast to the episomal state in their normal life-cycle, DNAs of high-risk HPVs are frequently found integrated into the host genome in invasive cervical cancer (ICC) [4,5]. Viral DNA integration leads to enhanced expression of two viral transforming genes, E6 and E7, which play critical roles in carcinogenesis [6,7].

In recent years next generation sequencing technologies have been increasingly incorporated into viral genomic research with the aim of comprehensively defining viral

genomic sequences in clinical samples [8]. HPV genomic research is no exception; the application of ultra high-throughput sequencing has been applied in the identification of known and unknown HPV genotypes in both cervical and cutaneous lesions [9-11]. In these studies, amplification of full-length HPV genome sequences from clinical specimens has been performed using unbiased amplification techniques such as rolling circle amplification or multiple displacement amplification with phi29 DNA polymerase, followed by deep sequencing analyses or next generation sequencing (NGS) [10,11].

In addition, the genetic diversity of viral quasispecies in infected cells or tissues, which is a typical characteristic of RNA viruses [12,13], has been extensively examined by employing deep sequencing techniques. RNA viral populations consist of 'mutant clouds', rather than genomes with the same nucleotide sequence, due to the fact that they utilize low-fidelity viral RNA polymerases for their genome replication. Viral quasispecies play major roles in many of the biological activities of RNA viruses. For example, their capacity to change cell tropism or host range or to overcome internal and external selective constraints, such as immune responses and antiviral agents, depends on the presence of variants in mutant clouds. Viral genomic diversity in individual clinical specimens has also been described among DNA viruses, including herpes simplex virus type 1 [14] and Epstein-Barr virus (EBV) [15]. Intriguingly, the detection of hypermutated HPV1a and HPV16 genome sequences in plantar warts and precancerous cervical biopsies, respectively, has also been reported [16]. However, the mutational landscape in the full-length HPV genome present in a clinical specimen and its physiological significance in viral carcinogenesis have not yet been investigated in a comprehensive manner.

In this study, we aimed to utilize NGS to analyze genetic variation in the entire HPV genome isolated from varying individual clinical samples. To this end, we have used a high-fidelity long-range PCR enzyme to amplify full-length HPV16 genomes from cultured cells and clinical samples. We report that PCR primers targeting a short region of the HPV16 genome yielded amplicons covering the entire viral genome sequence in a single reaction. By analyzing the amplified HPV16 DNA on the Illumina next generation sequencer, we have established a series of procedures for reconstructing the full-length HPV16 genome sequence and extracting genetic variations, such as nucleotide substitutions and insertions/deletions, from millions of short read sequences. This work could form the basis for a comprehensive analysis of HPV genetic variation present in individual clinical specimens.

Materials and Methods

Ethics Statement

Human cervical exfoliated cells were collected from patients at NTT Medical Center Tokyo with written informed consent. The study adhered to the declaration of Helsinki and was approved by the Ethics Committee at NTT Medical Center Tokyo.

Cell culture

W12 cell clones 20850 (5 to 50 copies of HPV16 episomes per cell) and 20863 (500 to 1,000 copies of HPV16 episomes per cell) were cultured in the presence of mitomycin C-treated 3T3m feeder cells as described previously [17,18]. CaSki and human embryonic kidney 293 (HEK293) cells were cultured at 37°C with 5% CO_2 in DMEM supplemented with 10% fetal bovine serum, 50 U/mL of penicillin, and 50 µg/mL of streptomycin.

Extraction of episomal and total DNA

To extract episomal HPV DNA from W12 cells, a modified Hirt method was used [19]. Briefly, subconfluent cells on a 6-cm dish were digested with 500 µL of lysis buffer consisting of 25 mM Tris-HCl (pH 7.5), 5 mM EDTA, 0.6% SDS, and 50 µg/mL of RNase A at room temperature for 5 min. After the addition of 350 µL of precipitation buffer consisting of 3 M CsCl, 1 M potassium acetate, and 0.67 M acetic acid, the solution was incubated on ice for 15 min, and precipitated by centrifugation (14,000 x g, 15 min, 4°C). Cleared supernatant was applied onto a Miniprep column (Favorgen, Ping-Tung, Taiwan) and passed through the column by centrifugation (14,000 x g, 1 min). The column was then washed with 750 µL of wash buffer consisting of 10 mM Tris-HCl (pH 7.5), 80 mM potassium acetate, 40 µM EDTA, and 60% ethanol. DNA was eluted with 60 µL of elution buffer consisting of 10 mM Tris-HCl (pH 7.5) and 0.1 mM EDTA. The resultant DNA fraction mainly contains extrachromosomal DNAs.

Total DNA was isolated from cervical exfoliated cells using the QIAamp DNA blood kit (QIAGEN, Hilden, Germany). The DNA samples were genotyped by PGMY-reverse blot hybridization assay [20,21], and HPV16-positive samples without other detectable HPVs from LSIL and ICC specimens were used for subsequent PCR. Total DNA was extracted from CaSki cells as described above for clinical samples. The concentrations of extracted DNAs were about 80 ng/µL from the cultured cells and 2 to 4 ng/µL from clinical samples.

Full-circle PCR

PCR was performed in 10 µL consisting of 1× PrimeSTAR® GXL Buffer (Takara, Ohtsu, Japan), 200 µM dNTP mixture, 0.25 µM forward primer, 0.25 µM reverse primer, 0.25 U of PrimeSTAR® GXL DNA polymerase (Takara), and 2 to 4 ng of template DNA. Primers used are as follows: 1742F, 5'-tgc tgt cta aac tat tat gtg tgt ctc-3'; 1873R, 5'-gcg tgt ctc cat aca ctt ca-3'; 1869F, 5'-cac gcc aga atg gat aca aa-3'; 1746R, 5'-cag caa ttt ttc aat tgt ttc tc-3'. Positions of 5'-end nucleotide of primers in the reference HPV16 genome (HPV16REF in Papillomavirus *Episteme*, http://pave.niaid.nih.gov) are used as primer names with either forward (F) or reverse (R) orientation. The plasmid containing the full-length HPV16 genome, HPV16/pUC19 [22], was used as a template for positive PCR. The PCR protocol was 98°C for 30 s, followed by 30 cycles of 98°C for 10 s, 60°C for 15 s, 68°C for 2 min. The PCR products were separated on a 0.7% agarose gel in 1 x TAE buffer and visualized with ethidium bromide.

Deep sequencing

Approximately 8-kb amplicons generated by full-circle PCR with the primer-pair 1742F/1873R were separated on a 0.7% agarose gel and purified using the Wizard gel purification kit (Promega, Madison, WI). To prepare DNA libraries compatible with Illumina NGS, the purified DNA (16 ng) was fragmented and adaptor-ligated using the Nextra DNA sample prep kit (Epicentre, Madison, WI), followed by DNA purification with the QIAquick PCR purification kit (QIAGEN). The resultant DNA libraries were amplified using a minimal PCR amplification step with Phusion High-Fidelity DNA polymerase (New England Biolab, Ipswich, MA) as follows: 72°C for 3 min, 95°C for 30 s, followed by 13 cycles of 95°C for 10 s, 62°C for 30 s, 72°C for 3 min. Adaptor-ligated DNAs in the range of 500 to 700 bp were then size-selected by 1% agarose gel electrophoresis and purified using the Wizard kit. Five to 8 libraries from different clinical samples were multiplexed with adaptors containing different index sequences and simultaneously subjected to deep sequencing. Cluster generation and sequencing were performed for 151 cycles on a MiSeq sequencer (Illumina, San Diego, CA) with the MiSeq Reagent kit (300 cycle) (Illumina) according to the manufacturer's instructions. Fluorescent images were analyzed using the Illumina MCS1.1/RTA1.13.56 base-calling pipeline to obtain FASTQ-formatted sequence data. To construct contiguous DNA sequences (contigs), total sequences of paired-end 151-mer reads were assembled using ABySS-pe v1.3.3 [23] with the following parameters: k80, n1200, c1000, t10, e10, q20, and s160; or k80, n120, c100, t10, e10, q20, and s160. The assembly generated 2 to 20 contigs, followed by further assembly of these sequences into the complete circular sequence by Phrap [24].

The fidelity of *de novo* assembly was examined by alignment of paired-end reads to the assembled sequence using Burrows-Wheeler Aligner (BWA) v0.6.1 [25]. Prior to read mapping, read sequences of Phred quality score ≥20 were selected by PoPoolation v1.2.2 [26], and trimmed for 20 bases at 5'-terminus and 51 bases at 3'-terminus because 5' and 3'-terminus of reads generate relatively low fidelity sequences. The processed 80-base sequences were mapped to the assembled sequence as a paired-end mode by BWA. The mapping results were visualized by Integrative Genomics Viewer (IGV) v2.0.34 [27] or Tablet v1.12.12.05 [28]. The numbers of paired-end reads obtained from each sample and used for *de novo* assembly are described in Table 1, and the average depth of the HPV16 genome ranged from x 7,624 for ICC sample 6 to x 48,221 for W12 sample. Nucleotide mismatches compared to the assembled reference genome and positions of SNPs in each sample were identified by using SAMtools v0.1.18 [29] with in-house Perl scripts (available upon request) or VarScan v2.3.2 [30]. Based on a quality score confidence threshold of Phred quality score > 30 (error probability ≤ 0.001) that was used to extract variation positions in the read sequences, we defined a position as homogeneous if the mutation frequency is < 0.5% and a position to be heterogeneous if the mutation frequency is > 0.5%. The presence of nucleotide substitutions and insertions/deletions was finally verified by visual inspection of mismatched read sequences using IGV and Tablet.

Table 1. *De novo* assembly of complete HPV16 genome sequences from short-read sequence data.

Sample	Cytology	Read number	Length (bp)	Variant lineage*	Average depth (per nucleotide)	DDBJ accession
W12	LSIL	2,539,664	7,904	EUR (A1)	48,221	
#1	LSIL	2,057,386	7,903	EUR (A3)	39,064	AB818687
#2	LSIL	1,739,070	7,906	EUR (A3)	33,020	AB818688
#3	LSIL	3,577,966	7,907	NA (D1)	36,233	AB818689
#4	LSIL	921,386	7,903	AFR2 (C)	17,495	AB818690
#5	LSIL	1,913,428	7,906	As (A4)	19,376	AB818691
#6	ICC	401,546	7,905	As (A4)	7,624	AB818692
#7	ICC	1,349,444	7,905	As (A4)	25,622	AB818693
CaSki	ICC	1,394,918	7,905	EUR (A1)	26,486	

*. Sublineage designations based on recent classification by Burk et al. [51] are in parenthesis.

doi: 10.1371/journal.pone.0080583.t001

Transient HPV16 replication assay

An HPV16 origin-positive plasmid was constructed by insertion of a *PstI* fragment of the HPV16 genome (from 7,005 to 7,906 and 1 to 880) into pGL4.50 (Promega). Expression plasmids for N-terminal FLAG-tagged HPV16 E1 and N-terminal FLAG-tagged HPV16 E2 were constructed by cloning of the codon-optimized cDNA of E1 and E2 into pCMV-β (Clontech, Palo Alto, CA). Expression plasmids for E1 mutants were generated by using the QuickChange Lightning Multi Site-Directed Mutagenesis Kit (Agilent Technologies, La Jolla, CA). Transient replication assays were performed as described by Fradet-Turcotte et al. [31] with some modifications. Briefly, HEK293 cells were plated 20 h before transfection in a 24-well plate at a density of 32,000 cells/well, and transfected with 2 ng of the origin-positive plasmid and 2 ng of pGL4.75 (Promega), together with 20 ng of the E2 expression plasmid and the indicated amounts of E1 expression plasmid using the FuGENE6 reagent (Promega). The total quantity of transfected plasmid DNA was adjusted to 100 ng with the empty plasmid p3xFLAG-CMV10 (Sigma-Aldrich, St. Louis, MO) as carrier DNA. At 72 h after transfection, firefly and *Renilla* luciferase activities were measured using the Dual-Glo Luciferase assay system (Promega) on an ARVO MX luminescence counter (PerkinElmer, Waltham, MA), and the level of replication was quantified as the ratio of the two luciferase activities.

Nucleotide sequence accession number

All assembled HPV genome sequences have been deposited in the DNA Data Bank of Japan (DDBJ) under accession numbers AB818687 to AB818693 for HPV16, AB819272 to AB819274 for HPV52, and AB819275 to AB819279 for HPV58. The sequence reads of the HPV

genomes are available from the DDBJ Sequence Read Archive under accession number DRA001083.

Results

Full-circle PCR amplifying full-length HPV16 genome sequences

Using PrimeSTAR® GXL polymerase, which is specifically designed for the fast and accurate amplification of long DNA sequences, and the HPV16-specific primers 1742F and 1873R, we generated two amplicons from HPV16/pUC19 plasmid DNA: a short fragment of ~130 bp and a large fragment consisting of the entire HPV16/pUC19 sequence of approximately 11 kb (with ~130-bp overlap) (Figure 1A, lanes 2 to 7, and see Figure 1B). This PCR reaction is slightly less efficient at creating the large amplicon than the same reaction using the non-overlapping primers 1869F and 1746R, which create only one amplicon (Figure 1A, lanes 9 to 14). The reactions with PrimeSTAR® GXL polymerase were both specific (only 1 or 2 PCR amplicons, depending on the primers used) and sensitive (we successfully amplified as little as 0.01 pg of input template DNA, which corresponds to about 900 copies of the plasmid). The introduction of cellular DNA did not inhibit this reaction, even at the sub-picogram level of template DNA (Figure S1).

Using the primer-pair 1742F/1873R and PrimeSTAR® GXL polymerase, we also amplified two DNA fragments from extrachromosomal HPV16 DNA isolated from W12 cells that were originally isolated from an LSIL biopsy (Figure 1C). The short and long amplicons matched the predicted sizes of 132 bp and ~8 kb, respectively (Figure 1B), and the long amplicon covered the complete HPV16 genome, as confirmed by Sanger sequencing (results not shown). Hence we refer to this overlapping PCR hereafter as full-circle PCR. To further test the utility of full-circle PCR with PrimeSTAR® GXL polymerase, DNA prepared from CaSki cells, known to contain 60 to 600 copies of integrated tandem repeated HPV16 genomes [32,33], was used as the PCR template. As expected, a mixture of 8 and 6.5-kb amplicons were obtained (Figure S2).

Importantly, full-circle PCR was able to generate approximately 8-kb amplicons using DNA isolated from HPV16-positive cervical exfoliated cells in patients with either LSIL (Figure 1D, lanes 2 to 6) or ICC (lanes 7 and 8). This observation prompted us to use these long PCR products for genetic variation analyses of full-length HPV16 genomes derived from clinical samples.

De novo assembly of full-length HPV16 genome sequences by deep sequencing

In order to comprehensively analyze HPV genetic variation through deep sequencing, we sought a methodology capable of determining the full-length reference sequence of the HPV16 genome from high-throughput short-read sequence data. First, to develop the system, the 8-kb DNA amplified from W12 DNA by full-circle PCR was fragmented and adaptor-ligated to yield a DNA library compatible with Illumina next generation sequencers. Deep sequencing of the resultant library generated sequence data from more than a million paired-end reads. *De novo* assembly of those paired-end reads by ABySS-pe and Phrap generated one contiguous sequence of 7,904 bp length, which was a perfect match for the full-length W12 HPV16 genome sequence in GenBank (accession No. AF125673). Next, the long PCR products from CaSki DNA were subjected to deep sequencing analysis. The *de novo* assembly procedure once again resulted in construction of one contiguous sequence of 7,905-bp length, identical to the full-length CaSki HPV16 genome sequence in GenBank (accession No. U89348). Mapping of the total read sequences to the CaSki reference sequence demonstrated the presence of two large deletions; from nucleotide positions 1 to 470 and 6,907 to 7,905 (Figure S3), which perfectly matched a deleted region previously reported in CaSki cells [33]. Thus, it is likely that the 6.5-kb DNA products obtained from CaSki DNA contain this 1,469-bp deletion. Overall, these results demonstrate the accuracy of long PCR, deep sequencing and bioinformatics to obtain full-length HPV16 genome sequences.

To determine the complete genome sequence of HPV16 contained in clinical specimens, we analyzed the 8-kb full-circle PCR products from 7 clinical samples by deep sequencing and assembled the complete viral genome sequence as described above. Table 1 presents the results of this analysis and demonstrates that *de novo* assembly yielded one contiguous sequence for each sample. The length of each sequence ranged from 7,903 to 7,907 bp due to the differences in the length of the non-coding region between E5 and L2 (Figure S4).

The HPV16 genome is classified into 4 major variant-lineages based on a unique combination of single nucleotide polymorphisms (SNPs): European-Asian, including the sublineages European (EUR) and Asian (As), African 1 (AFR1), African 2 (AFR2), and North-American/Asian-American (NA/AA) [34]. As presented in Table 1, SNP analysis of the assembled HPV16 genomes assigned the following variants to each clinical sample: 2 LSIL samples, EUR; 1 LSIL sample, NA; 1 LSIL sample, AFR2; and 1 LSIL and 2 ICC samples, As. Furthermore, phylogenetic tree analysis with the assembled complete genome sequences of HPV16 confirmed the assignments in variant-lineages (Figure S5). These results indicate that one HPV16 variant predominates in each clinical specimen.

Analysis of nucleotide variations in HPV16 genomes

Before analyzing the sequence variation present in clinical samples, we first validated the efficacy and error rates of deep sequencing on our platform. For this purpose, we used a linearized full-length HPV16 DNA that was excised from HPV16/pUC19 by *Bam*HI digestion. The read sequences obtained were aligned to the prototype HPV16 sequence (GenBank accession No. K02718), and the number of reads containing nucleotide mismatches was determined at each position of the viral genome. This analysis enabled us to calculate mutation frequencies at each nucleotide position (the average depth of reads count per nucleotide position was 7,035). As shown in Figure 2, an overall profile of the mutation/error frequency demonstrated an error rate below 0.3% distributed throughout the whole sequence, which reflects

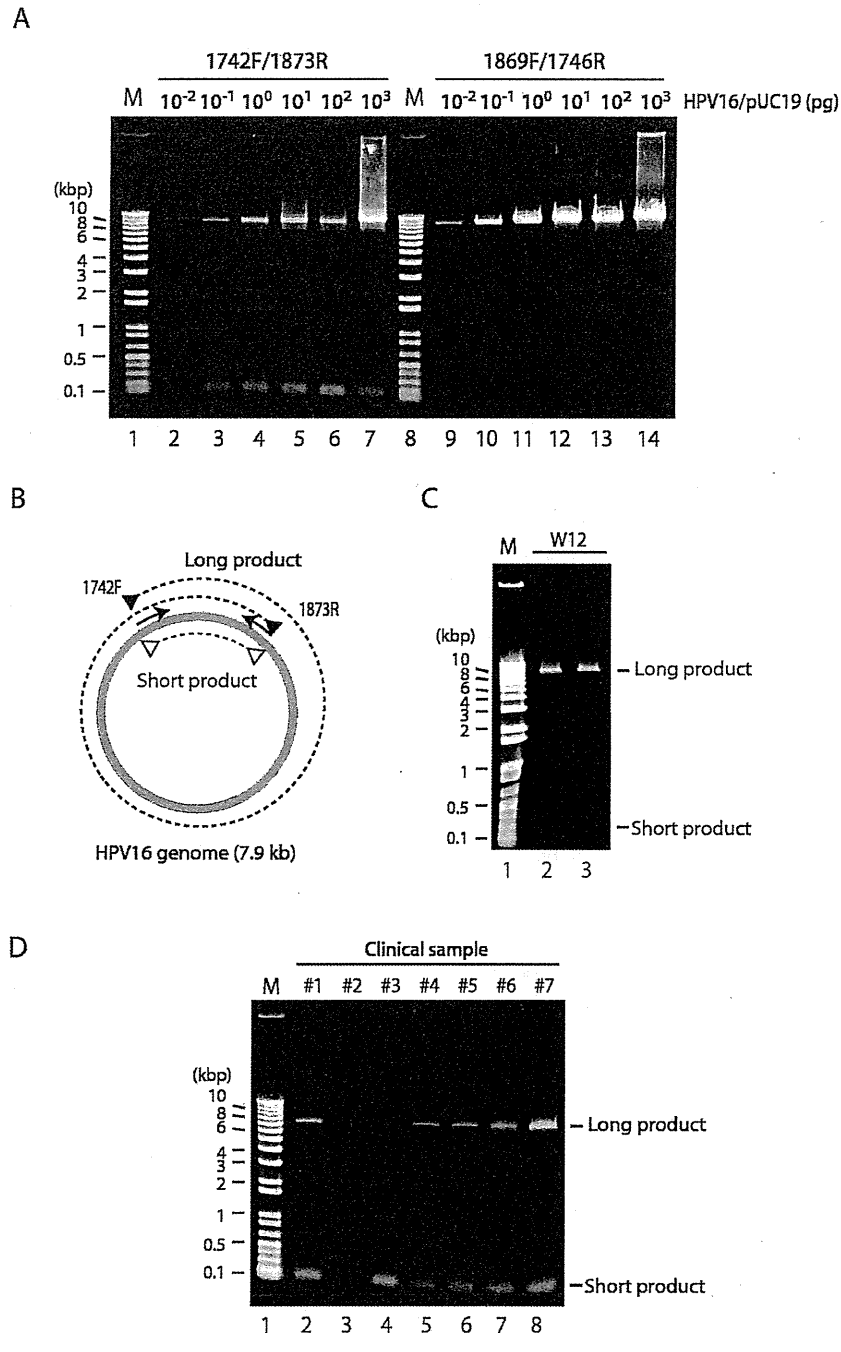

Figure 1. Amplification of full-length HPV16 genomes by full-circle PCR. (A) PCR was performed with PrimeSTAR® GXL DNA polymerase and HPV16-specific primer-pairs as indicated. The amounts of HPV16/pUC19 used for the PCR template are also indicated above. The PCR products were analyzed by agarose gel electrophoresis. M, DNA size markers. (B) Scheme for full-circle PCR. PrimeSTAR® GXL DNA polymerase generates short and long DNA products with primer-pair 1742F/1873R. (C) Full-circle PCR with DNA extracted from W12 cells, clone 20863 (high-copy HPV16 episomes) (lane 2) and clone 20850 (low-copy HPV16 episomes) (lane 3). M, DNA size marker (lanes 1) (D) Full-circle PCR using DNA isolated from 7 clinical specimens: 5 LSIL (lanes 2 to 6), and 2 ICC (lanes 7 and 8). M, DNA size marker (lanes 1).

doi: 10.1371/journal.pone.0080583.g001

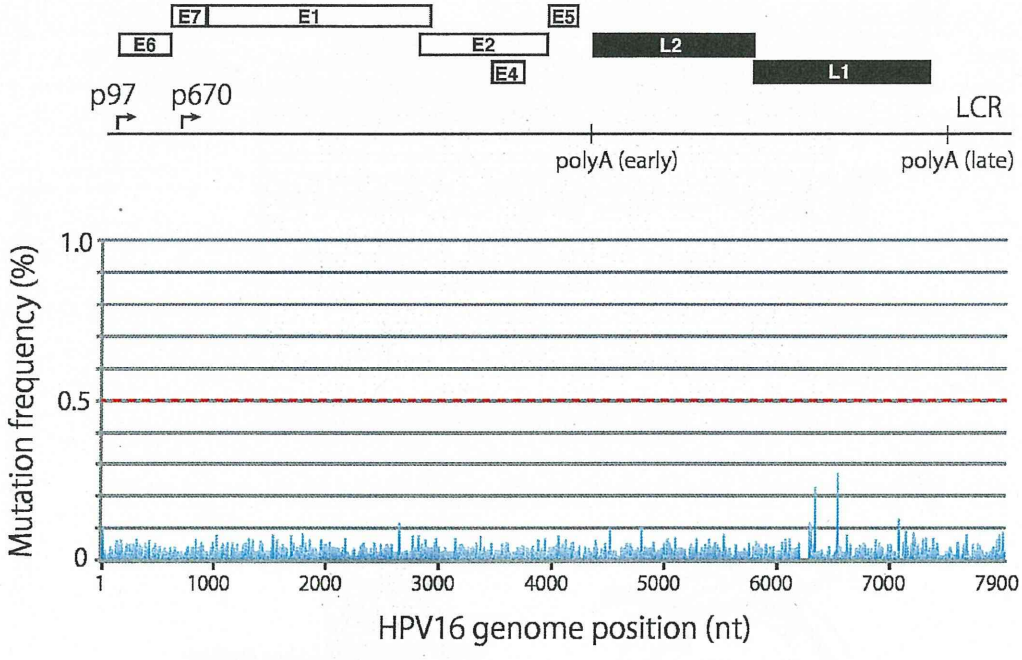

Figure 2. Mutation frequency profile of full-length HPV16 genomes prepared from a plasmid. The read sequences obtained with full-length HPV16 genomes prepared from a cloned plasmid were aligned to the reference HPV16 sequence, and mutation/error frequencies at each nucleotide position relative to the total coverage (number of reads that encompass each nucleotide, up to the maximum x 8,000) are presented in the landscape of the full-length HPV16 genome. A threshold line for a reliable mutation frequency (0.5%) is indicated with the red dotted line. The genome organization of HPV16 is indicated above: p97, the early promoter; p670, the late promoter; polyA(early) and polyA(late), the early and late polyadenylation signals, respectively.

doi: 10.1371/journal.pone.0080583.g002

intrinsic errors generated in the deep sequencing analysis. The average error rate per nucleotide position throughout the whole sequence was determined to be 0.0070%. Visualization and manual inspection of aligned read sequences revealed that the two minor peaks observed at nt positions 6,242 and 6,434 (see Figure 2) were derived from mis-mapping of reads to ends of the linear HPV16 DNA (*Bam*HI site, at nt 6,154).

Our deep sequencing analysis of HPV16 DNA amplified by PrimeSTAR® GXL polymerase demonstrated that the average error rate was 0.0076% (results not shown), which is comparable to the error rate reported by the manufacturer (0.0062%), indicating high fidelity DNA amplification by this polymerase. Based upon this low error rate and our analytical method's ability to pick up nucleotide variation with a minimum confidence score threshold of Phred quality score 30 (error probability $\leq$ 0.001), we decided to use 0.5% as a threshold value of mutation frequency to distinguish real mutations from putative errors.

We applied this variation analysis method to HPV16 genome sequences obtained from W12 cells. As shown in Figure 3, alignment of the paired-end reads to the W12 reference sequence revealed no major nucleotide substitutions with a frequency >0.5% in the read coverage , suggesting that HPV16 genome sequences are highly homogeneous in W12 cells.

Next we employed this established analysis procedure to examine HPV genomic variation in clinical samples. We report two types of mutation profiles found in 7 clinical samples: a highly homogeneous profile as observed with W12 cells, and a profile with 1 to 3 specific positions of nucleotide substitution. Four samples (#1, #4, #5, and #7) showed an almost homogeneous profile without specific nucleotide substitution (two representative profiles are presented in Figure S6) and 3 samples (#2, #3, and #6) demonstrated a mutation profile with several positions of nucleotide substitution (Figure 4). The nucleotide substitutions were located in the early region of the HPV16 genome, E6 and E1, and the non-coding region between E5 and L2, with frequencies from 0.60 to 5.42% (Table 2). Intriguingly, the nucleotide substitutions observed in the E1 gene of sample 6 cause amino-acid (aa) changes in the E1 protein: methionine at aa position 326 to isoleucine, and glutamine at aa position 381 to glutamic acid. The nucleotide substitution in the E6 gene detected in sample 6 also leads to an aa change in the E6 protein, glutamic acid to aspartic acid at aa position 25.

We were also able to employ our full-circle PCR and deep sequencing approach to analyze clinical samples that contained HPV52 and HPV58 DNA (Figure S7 and Table S1), suggesting that this method is not specific to the analysis of

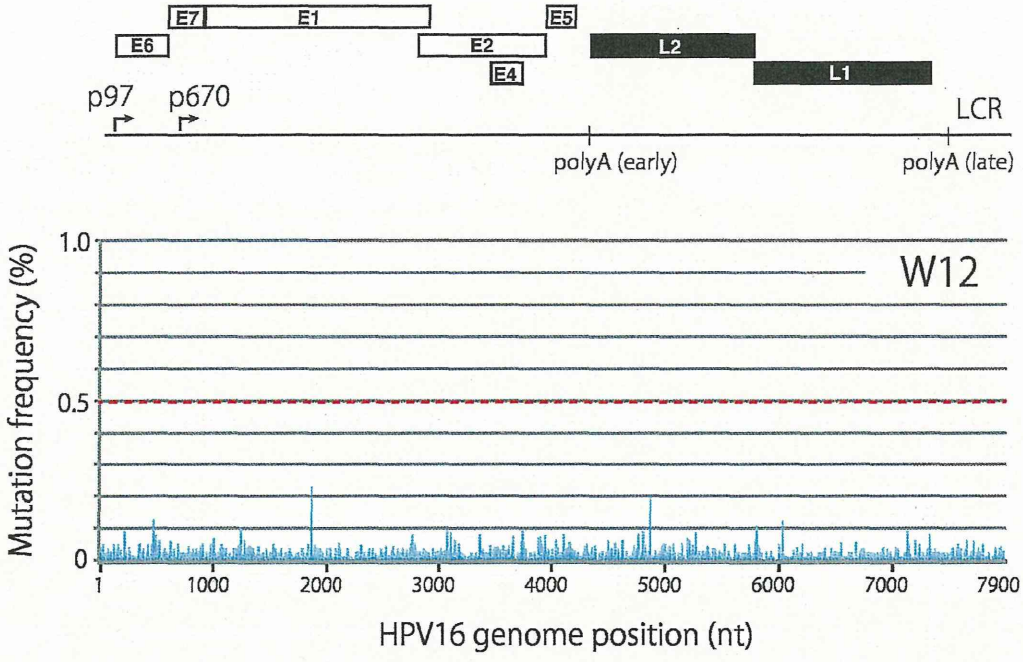

Figure 3. Mutation frequency profile of full-length HPV16 genomes in W12 cells. The read sequences obtained with full-length HPV16 genomes prepared from W12 cells were aligned to the reference HPV16 sequence (AF125673), and mutation/error frequencies at each nucleotide position are presented in the landscape of the full-length HPV16 genome. A threshold line for a reliable mutation frequency (0.5%) is indicated with the red dotted line. The genome organization of HPV16 is indicated above.
doi: 10.1371/journal.pone.0080583.g003

HPV16 and that it is also applicable to the oncogenic HPV types prevalent in East Asian countries including China and Japan [35-37].

Effect of E1 amino-acid changes on its replication function

The *de novo* assembled HPV16 genomes from clinical specimens revealed aa polymorphisms of the E1 protein in its DNA-binding domain at aa positions 294 and 326: a replacement of leucine (prototype) at position 294 with methionine (L294M) in 2 LSIL specimens (#3 and #4) and that of isoleucine (prototype) at position 326 with methionine (I326M) in all the specimens (Figure 5A). Further, nucleotide variation analyses showed a novel aa variation at position 381 from glutamine (prototype) to glutamic acid (Q381E) in sample 6. To explore the biological significance of these E1 variations, we mutated the corresponding aa residues in the European prototype E1 protein and tested the mutated E1's ability to support HPV16 origin-dependent DNA replication. The E1 mutant Y379F (in which tyrosine at 379 is replaced with phenylalanine), which is expected to lose replication activity as reported previously [38], was also included as a representative of a replication-deficient E1 protein.

In the transient HPV16 replication assay, two reporter plasmids were transfected into HEK293 cells together with expression vectors for FLAG-tagged E1 and E2. Firefly luciferase (Fluc) is expressed from the HPV16 origin-positive plasmid, whereas *Renilla* luciferase (Rluc) is expressed from the origin-deficient plasmid, so the ratio of the two luciferase activities (Fluc/Rluc) in the presence of the E1/E2 expression vectors represents levels of HPV origin-dependent replication. As previously reported [31], the Fluc/Rluc ratio obtained with the origin-positive plasmid increased in a manner dependent on the amount of the E1 expression plasmid (Figure 5B). Under these assay conditions, two E1 variants, L294M and I326M, showed replication activities almost comparable to the parental E1 (Figure 5C). In contrast, Q381E exhibited a reduced activity for supporting HPV16 replication, and Y379F completely lost the replication activity as expected. Western blot analyses revealed that the expression levels of I326M, Q381E, and Y379F were comparable to that of the prototype E1 (Figure 5D), indicating that the reduced replication activity of Q381E is not due to reduced protein level.

Detection of deletions in HPV16 genomes

Because our deep sequencing analysis was able to precisely define the deletion in the HPV16 genome of CaSki cells, we examined HPV16 genome deletions in the 7 clinical samples by read mapping to the assembled reference sequence. Of the 5 LSIL samples, 4 LSIL samples did not show any deletions

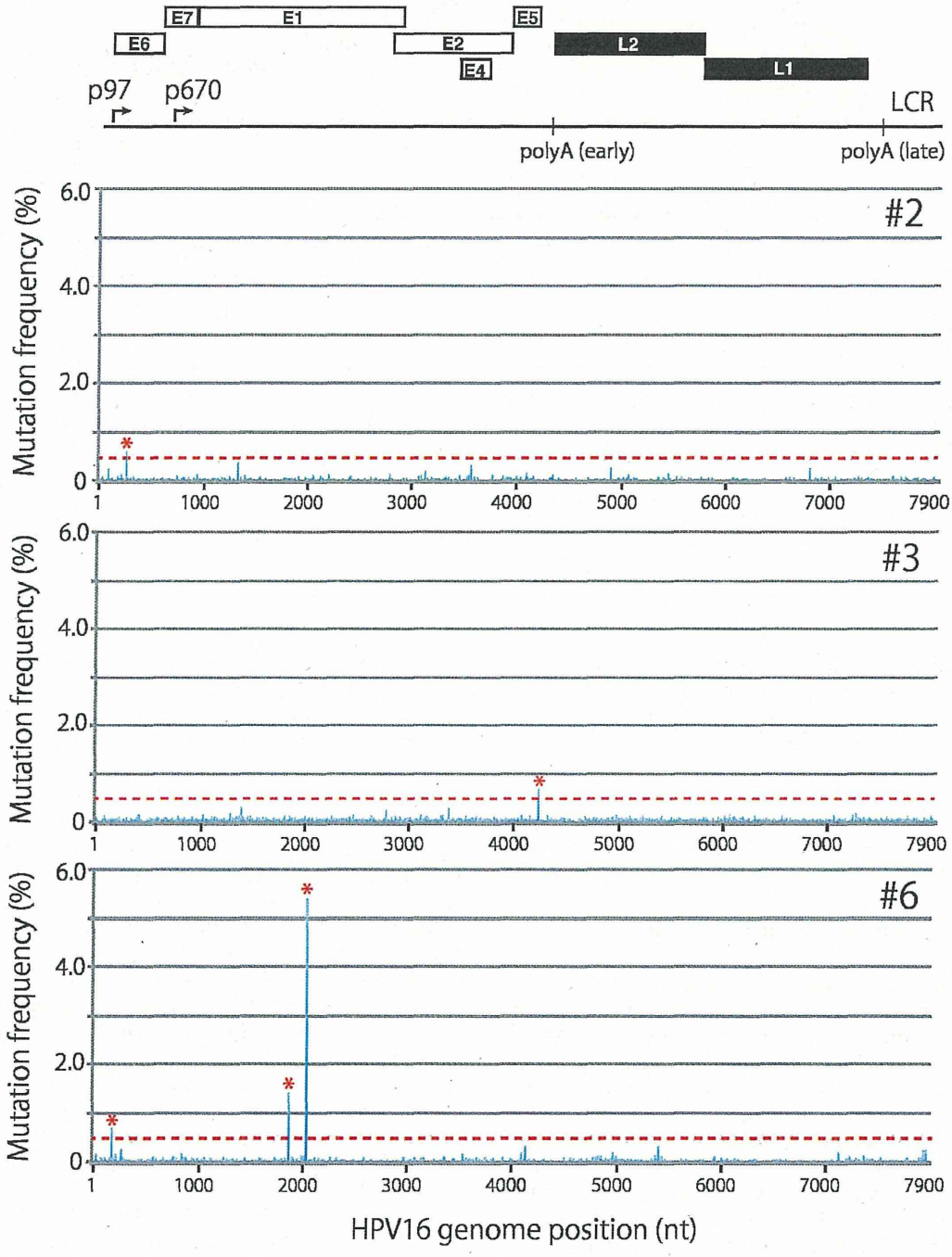

Figure 4. Mutation frequency profile of full-length HPV16 genomes in clinical specimens. The read sequences obtained with full-length HPV16 genomes prepared from clinical specimens (2 LSIL samples, #2 and #3; 1 ICC sample, #6) were aligned to their *de novo* assembled complete genome sequences, and mutation/error frequencies at each nucleotide position are presented in the landscape of the full-length HPV16 genome. A threshold line for a reliable mutation frequency (0.5%) is indicated with the red dotted line. Peaks above 0.5% are indicated with red asterisks. The genome organization of HPV16 is indicated above.

doi: 10.1371/journal.pone.0080583.g004